STUDY OF EXOTIC NUCLEI IN THE FLEROV LABORATORY OF NUCLEAR REACTIONS AT JOINT INSTITUTE FOR NUCLEAR RESEARCH*

Yu.L. Parfenova

for the ACCULINNA-2 Collaboration

G.N. Flerov Laboratory of Nuclear Reactions, JINR, 141980 Dubna, Russia

(Received January 3, 2018)

The fragment separator ACCULINNA-2 has been constructed, approved by the Programme Advisory Committee (PAC) and commissioned in the G.N. Flerov Laboratory of Nuclear Reactions (JINR, Dubna) in 2017. It was tested with the ^{15}N beam at the energy of 49.7 MeV/nucleon. The secondary beams ^{6}He and ^{12}Be produced in the beryllium target were obtained with purities and intensities predicted by the code LISE++. Here, we list the most meaningful and challenging experiments on the light drip-line nuclei at ACCULINNA, which should be clarified at ACCULINNA-2: *(i)* the search for the minor $2p$-decay branch of the first excited state of ^{17}Ne, the $\Gamma_{2p}/\Gamma_{\gamma}$ width ratio; *(ii)* study of break down of the shell closure in the doubly magic ^{10}He in the ^{3}H(^{8}He,p)^{10}He reaction; *(iii)* study of the β-delayed proton emission in ^{26}P and ^{27}S, which offers insight into the structure of the initial and the final states of these exotic nuclei. Among the first-day experiments is a study of the low-energy resonance states of ^{7}H anticipated for the $4n$ decay.

DOI:10.5506/APhysPolB.49.495

1. Introduction

Radioactive ion beams (RIBs) supplied by the ACCULINNA separator [1] proved their worth as a reliable tool in the study of light drip-line nuclei carried out in Dubna during the last 20 years [2]. Though light nuclei up to Mg occupy a relatively small part of the nuclear chart, they are a topic of challenging work in the contemporary nuclear physics. For both neutron- and proton-rich nuclei, stability limits are reached here and for some of these nuclei new aspects of nuclear dynamics become evident (see review [3] and references therein).

* Presented at the XXXV Mazurian Lakes Conference on Physics, Piaski, Poland, September 3–9, 2017.

In particular, in the vicinity of the drip lines, clustering becomes a common phenomenon, and nuclei with a far extended neutron halo can be found here. Among them, one encounters one-neutron (^{11}Be) and two-neutron (^{6}He, ^{8}He, ^{11}Li, ^{14}Be) halo nuclei. The pairing effect sharply comes out at the stability borders resulting in specific effects, *i.e.* the appearance of borromean nuclei, two-proton radioactivity and the true three-body (democratic) decay. Inherent to the borromean halo nuclei is the emergence of the so-called soft excitation modes.

Considering the neutron drip-line nuclei, we notice that versatile and reliable data should be obtained elucidating the spectra of ^{10}He and its neighbors. The breakdown of the $N = 8$ magic number observed for the ^{10}He nucleus makes this study urgent. Another challenge is the possible existence of novel types of radioactivity, such as the two-neutron and four-neutron radioactive decay, which perhaps could be discovered for some nuclei near the neutron drip line. In the search for the $2n$ radioactivity, the nuclei of interest are ^{16}Be and ^{26}O. The ^{7}H and ^{28}O nuclei are candidates for $4n$ radioactivity.

Very neutron-deficient nuclei exhibit β decay, and it becomes an important tool in studies of these nuclei offering insight into the structure of the initial and the final states. Due to the large decay energy, unbound states in the daughter nuclei can be populated, followed by emission of β-delayed charged particles. Since detection of such particles is easier and more efficient than detection of γ rays, they represent a valuable source of information, particularly for the most exotic nuclei which are usually produced in small quantities. On the other hand, the complete knowledge of the decay scheme, including all particle emission channels, is required for the correct determination of the β strength, which bears structural information. Some delayed particle emission channels have an additional advantage when they represent a reverse process to the radiative capture reaction of astrophysical significance. For example, the β-delayed proton emission ($\beta\, p$) can be used to characterize a resonance playing a key role in the $(p\,,\gamma)$ reaction. This is especially worthwhile when the study of the direct reaction is hampered by the low intensity of the radioactive beam. In this context, the decay study of ^{16}P and ^{27}S is of interest. Both decays contribute to the complete understanding of the nucleosynthesis of ^{26}Al, which is a cosmic γ-ray emitter observed in the interstellar medium by satellite-based γ telescopes [3]. In high-temperature environments, like in novae explosions, ^{26}Al is produced by the reaction chain ^{24}Mg(p,γ) ^{25}Al$(\beta+,\nu)$ ^{25}Mg(p,γ) ^{26}Al [4]. However, this sequence can be bypassed by the proton capture reactions ^{26}Al(p,γ) ^{26}Si(p,γ) ^{27}P [4]. One way to constrain the rates of these reactions is by the study of β decay of ^{26}P and ^{27}S, respectively, followed by a delayed emission of protons and γ rays.

2. The ACCULINNA fragment separator

Technical parameters of the fragment separation ACCULINNA are substantially constrained compared to those of other facilities. The available RIBs are limited to the nuclei with $Z < 20$, the maximal energy is $E <$ 40 MeV/nucleon. However, the ACCULINNA facility has its advantages. The record-high intensity of primary beams of the U-400M cyclotron (up to 5 $p\mu$A) provides quite high intensities of exotic nuclei with lower energies, compared to other facilities. The typical energy of RIBs at the separator ACCULINNA is about 20–35 MeV/nucleon, which is optimal for nuclear structure studies manifesting itself in direct processes of nuclear interaction, *i.e.* in elastic and inelastic scattering, in transfer, charge-exchange reactions, and also in reactions of quasi-free scattering.

These circumstances together with modern experimental setups and methods of data analysis including theory development, allowed obtaining of the whole set of world-class results with the ACCULINNA facility.

3. The ACCULINNA-2 fragment separator

ACCULINNA-2 is designed and constructed [4, 5] to be a more effective substitute for the ACCULINNA separator. The primary heavy-ion beam of the U-400M cyclotron is focused on the production target located at the beginning of the main separator section. This is an achromatic ion-optical structure having one dispersive focal plane, where a wedge-shaped beryllium degrader is placed. The RIB nuclei, cleaned from the primary beam ions and from the majority of other reaction products, are focused on the final achromatic plane situated outside the cyclotron hall in a room free of radiation created by the primary beam. Guided by the quadrupole magnets of the separator third section, the RIB nuclei run to the physics target. A long 14-meter flight base allows for the time-of-flight measurement to give the energy of individual RIB nuclei ascertained with one-percent accuracy. Also, the magnetic structure of this section is optimized for the installation of an RF filter, which is planned for 2018. Position-sensitive chambers (MWPC or PPAC) installed at the end part of this section will measure the inclination angles of individual nuclei hitting the target with accuracy 3–4 mrad.

Increased apertures of magnets employed in the new separator offer RIB intensities increased by 30 times as compared to those obtained with ACCULINNA, see Table I. Better momentum resolution granted for the separated RIBs suggests their improved purity. The characteristics expected for some RIBs which will be obtained from the ACCULINNA-2 separator are presented in Table I. The RIB energies, E, given there, represent some typical choices available for the set of primary beams accelerated at

the U-400M cyclotron. The RIB intensities, I, and their purity, P, were calculated using the LISE++ code [6, 7]. Note that the beam intensities available at ACCULINNA-2 are approximately 25 times greater than those at ACCULINNA.

TABLR I

Characteristics for RIBs obtained for ACCULINNA and ACCULINNA-2. The beam energies (E) are given in MeV/nucleon; the fluxes (I) are given in pps. The secondary beam purities (P) are given in percents.

Primary beam		Secondary beam						
			ACCULINNA-2			ACCULINNA		
Ion	E	Ion	E	I	P	E	I	P
^{11}B	32	^{8}He	26	3×10^5	90	25	1×10^4	95
^{15}N	49	^{8}He	37	2×10^5	99	40	1×10^4	92
^{15}N	49	^{11}Li	37	3×10^4	95	37	2×10^3	40
^{18}O	33	^{14}Be	26	6×10^3	50	27	3×10^2	20
^{22}Ne	44	^{18}C	35	4×10^4	30	36	5×10^3	60
^{10}B	39	^{7}Be	26	8×10^7	90	38	1×10^6	50
^{20}Ne	53	^{18}Ne	34	2×10^7	40	40	5×10^4	15
^{20}Ne	53	^{17}Ne	35	1×10^6	10	42	3×10^3	3
^{32}S	52	^{24}Si	32	2×10^4	5	40	1×10^2	1

In March 2017, the ACCULINNA-2 facility has been tested with the ^{15}N beam at the energy of 49.7 MeV/nucleon. Secondary beams ^{6}He (with $E = 31.5$ MeV/nucleon, $I = 2.7 \times 10^3$, $P = 53\%$) and ^{12}Be (with $E = 39.4$ MeV/nucleon, $I = 1.9 \times 10^2$, $P = 92\%$) produced in the beryllium target have been obtained. Both the purities and intensities and also the sizes and shapes of the beam in the initial and final focal planes of ACCULINNA-2 are in a good agreement with those predicted by the code LISE++ [6, 7]. Further data analysis is in progress now.

Below, we list the most recent results obtained with ACCULINNA, which need clarification and further refinement at the ACCULINNA-2 facility.

3.1. Breakdown of shell closure in ^{10}He

In the past, it could be natural to suppose that ^{10}He is the next double magic nucleus after ^{4}He. This opinion stimulated numerous experiments [13–20] carried out since 1994 in attempt to obtain this helium isotope. The first paper reporting the ^{10}He discovery was published in 1994 [13]. Thus in Refs. [13–16], the observed wide peak between 1 and 1.5 MeV was explained as the ^{10}He ground-state resonance.

However, another interpretation related to the reaction mechanism can be suggested for these types of ^{10}He spectrum population [17, 18].

In our experiments [19, 20], ^{10}He was produced in the ^{3}H(^{8}He,p)^{10}He reaction. The obtained missing-mass spectrum of ^{10}He is shown in Fig. 1. In addition to the recoil proton, the ^{8}He nucleus emitted in coincidence was detected. This provided information about the ^{8}He emission angle ($\Theta_{8\mathrm{He}}$) and about the part ($\varepsilon = E_{nn}/E_{\mathrm{T}}$) of the ^{10}He center-of-mass total decay energy (E_{T}) going to the relative motion in the $2n$ subsystem ($\Theta_{8\mathrm{He}}$ is measured in respect to the momentum-transfer vector obtained from the proton emission angle). The ranges marked A, B, and C in the ^{10}He spectrum are characterized by the strongly pronounced angular and energy correlations. The analysis done for these correlations ensured us that the wide ($\Gamma > 1$ MeV) 0^{+} ground-state resonance of ^{10}He is located at $E_{\mathrm{T}} \simeq 2.2$ MeV. This state appears to be practically pure in the measured ^{10}He spectrum. In the range of $4.5 < E_{\mathrm{T}} < 6.0$ MeV, mainly the first excited 1^{-} state of ^{10}He contributes to the measured spectrum, and at $E_{\mathrm{T}} > 6.0$ MeV, the yield of the next 2^{+} state incerases. The order of the excited states is anomalous. Thus, for even–even nuclei with the neutron number $N = 8$ near the stability line (^{14}C, ^{18}O), the state 1^{-} is higher than the ground state by 6–7 MeV. The appearance of the 1^{-} intruder state in the ^{10}He spectrum is an evidence that the closed-shell structure breaks down in the case of this "doubly-magic" nucleus.

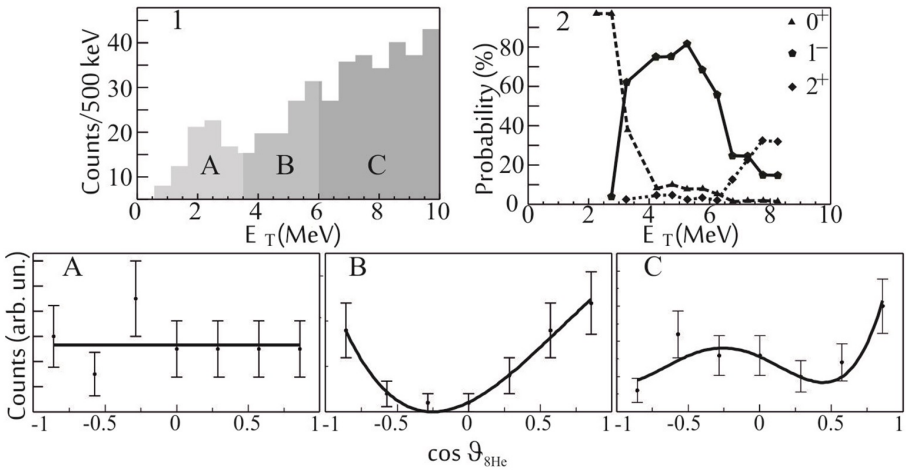


Fig. 1. The $2n$ transfer reaction ^{3}H(^{8}He,p)^{10}He as studied in Refs. [19, 20]. (1) Missing mass spectrum obtained for the ^{10}He nucleus; (2) Squared amplitudes of coherent s-, p-, d-wave contributions deduced from the angular distributions of ^{8}He appearing at the ^{10}He decay. The lower three panels show these angular distributions averaged over the energy ranges marked A, B, and C in panel 1.

The significance of getting more knowledge about the ^{10}He structure, including a deeper insight into its excitation spectrum, makes the relevant experiments to be in the priority list of works planned for the RIBs provided by ACCULINNA-2. This will be the study of the ^{3}H(^{8}He,p)^{10}He reaction aimed to acquire data exceeding by two orders of magnitude the statistics presented in Fig. 1. The ^{10}He spectrum populated in the ^{3}H(^{8}He,p)^{10}He reaction will be analyzed using the procedure suggested in Ref. [21] for the ^{5}H studies.

3.2. Search for the 2p decay branch of the first excited state in ^{17}Ne

True $2p$ decay from the ground state (see review [8]) has been observed for many nuclei, but there is only one nuclide where such decay takes place from an excited state, namely ^{17}Ne. The energy of the 1288 keV, $J^{\pi} = 3/2^{-}$ first excited state of ^{17}Ne exceeds the threshold of $2p$ emission only by 344 keV, whereas the proton emission from this state is not allowed. Experimental observation of $2p$ emission from the ^{17}Ne first excited state is impeded by the very small branching ratio with the competing γ-decay channel. Previous searches for the $2p$ decay mode of this ^{17}Ne state gave only a limit for $\Gamma_{2p}/\Gamma_{\gamma} \leq 7.7 \times 10^{-3}$ [10], while the theory [11] predicts a value of $\Gamma_{2p}/\Gamma_{\gamma} \simeq 2 \times 10^{-6}$.

An experiment aimed at searching for the ^{17}Ne first excited state $2p$ decay was conducted at the ACCULINNA facility [22]. In comparison with previous works, this experiment had two serious methodological improvements. First of all, the neutron transfer reaction ^{1}H(^{18}Ne, d)^{17}Ne was used to populate ^{17}Ne excited states. This reaction gives the highest possible relative yield of $J^{\pi} = 3/2^{-}$ state. In conjunction with the original approach developed for secondary beam experiments, namely the combined-mass method, this allows to achieve the new upper limit for $\Gamma_{2p}/\Gamma_{\gamma} \leq 1.6(3) \times 10^{-4}$. For the $2p$ branch of the first excited state of ^{17}Ne this little, but still measurable, $\Gamma_{2p}/\Gamma_{\gamma}$ implies that the reaction channel having cross section $\mathrm{d}\sigma/\mathrm{d}\Omega \simeq 1$ nb/sr becomes open to study. The use of ACCULINNA-2 allows for better purity, higher acceptance, and beam intensities 20 times exceeding those at ACCULINNA. This gives possibilities for us to achieve statistics for measurements of the branching ratio of about 10^{-6}, comparable with the theoretical limit from Ref. [11].

The problem of ^{17}Ne has important astrophysical consequences. The $\Gamma_{2p}/\Gamma_{\gamma}$ branching ratio is one of the parameters that determine radiative $2p$ capture by ^{15}O, one of the possible paths bypassing the ^{15}O waiting point in the rp process [9]. This is only a part of the general problem of explosive hydrogen burning in astrophysics which requires knowledge about $\Gamma_{p,2p}/\Gamma_{\gamma}$ branching ratios. The approaches used in Ref. [22] promise the opportunity to measure the extremely small $\Gamma_{p,2p}/\Gamma_{\gamma}$.

3.3. β-delayed proton emission from ^{26}P and ^{27}S

Delayed emission of protons following β decay of neutron-deficient nuclei ^{26}P and ^{27}S was investigated [23] at the ACCULINNA separator. Ions of interest, identified in flight, were implanted into the active volume of the gaseous optical time-projection chamber, which allowed us to record tracks of charged particles emitted in the decay. Total branching ratios for β-delayed proton emission and for β-delayed two-proton emission were determined. In addition, energy spectra for delayed protons below 2 MeV were established. Our findings for ^{26}P agree with the results of previous experiments. In the case of ^{27}S, however, the observed probability of delayed proton emission is an order of magnitude larger than that reported in literature. Two new strong proton transitions were identified, representing decays of the first two excited states of ^{27}P to the ground state of ^{26}Si.

The exact energies of the relevant resonances and the probability ratios of γ-to-proton emission can be established accurately using a compact telescope of silicon detectors surrounded by an array of germanium detectors. Thus, the most advantageous approach would combine results provided by both complementary techniques.

4. Nearest scientific plans for ACCULINNA-2 RIBs

All the problems listed above are urgent for study, so a priority order of the various scientific objectives needs to be established for the first use of the new ACCULINNA-2 facility.

The ^{6}H in the $^{6}He + d$ interaction. A probable choice for the first, demonstration experiment is the study of elastic and inelastic scattering, and neutron transfer in the ^{6}He+d interaction, with correlation analysis of the recoil proton from the deuterium target and decay products (^{6}He and α-particles). Study of the elastic scattering allows for getting the optical model parameters, and the low-lying resonant states can be investigated in the elastic scattering.

The ^{10}Li in the $d(^{11}Li,^{3}He)^{10}Li$ reaction. The low-energy structure (s-wave and p-wave states) of ^{10}Li is supposed to be studied in the $d(^{11}$Li,^{3}He$)^{10}$Li reaction at the energy of 25 MeV/nucleon in full kinematics using the combined mass method.

Study of ^{7}H and the 4n-decay problem. The two reactions ^{2}H(^{8}He,^{3}He)^{7}H and ^{2}H(^{11}Li,^{6}Li)^{7}H are suitable for the study made with the beams of ^{8}He and ^{11}Li obtainable from ACCULINNA-2, see Table I. The energies of these beams, 37–40 MeV/u, are optimal for reaching the maximum cross sections available for reactions notable for their rather large negative Q-values. In this study, the missing mass spectrum will be observed (^{3}He or ^{6}Li recoils assumed to be recorded in the reactions ^{2}H(^{8}He,^{3}He)^{7}H or ^{2}H(^{11}Li,^{6}Li)^{7}H, re-

spectively). To get more information on the α-transfer in the ^{2}H(^{11}Li,^{6}Li)^{7}H reaction, we will firstly investigate the ^{2}H(^{12}Be,^{6}Li)^{8}He. Similarly, the study of the ^{2}H(^{6}He,^{3}He)^{5}H is a tool for the main run of the ^{2}H(^{8}He,^{3}He)^{7}H reaction.

This work was supported by the Russian Science Foundation (grant No. 17-12-01367).

REFERENCES

[1] A.M. Rodin *et al.*, *Nucl. Instrum. Methods Phys. Res. B* **204**, 114 (2003).
[2] ACCULINNA web page, JINR, `http://aculina.jinr.ru/`
[3] L.V. Grigorenko *et al.*, *Physics-Uspekhi* **59**, 321 (2016).
[4] A.S. Fomichev *et al.*, JINR Communication E13-2008-168, JINR, 2008.
[5] W. Beekman *et al.*, Proc. of 13$^{\text{th}}$ Intern. Conf. on Heavy Ion Accelerator Technology, `www.nishina.riken.jp/hiat2015`, p. 33.
[6] O. Tarasov, D. Bazin, *Nucl. Instrum. Methods Phys. Res. B* **266**, 4657 (2008).
[7] `http://lise.nscl.msu.edu/lise.html`
[8] M. Pfützner *et al.*, *Rev. Mod. Phys.* **84**, 567 (2012).
[9] J. Görres, M. Wiescher, F.-K. Thielemann, *Phys. Rev. C* **51**, 392 (1995).
[10] M.J. Chromik *et al.*, *Phys. Rev. C* **66**, 024313 (2002).
[11] L.V. Grigorenko, M.V. Zhukov, *Phys. Rev. C* **76**, 014008 (2007).
[12] M.S. Golovkov *et al.*, in: EXON-2014 Proceedings, (Eds.) Yu.E. Penionzhkevich, Yu.G. Sobolev, Singapore, World Scientific, 2015, p. 171.
[13] A.A. Korsheninnikov *et al.*, *Phys. Lett. B* **326**, 31 (1994).
[14] H.T. Johansson *et al.*, *Nucl. Phys. A* **842**, 15 (2010).
[15] H.T. Johansson *et al.*, *Nucl. Phys. A* **847**, 66 (2010).
[16] Z. Kohley *et al.*, *Phys. Rev. Lett.* **109**, 232501 (2012).
[17] L.V. Grigorenko *et al.*, *Phys. Rev. C* **82**, 014615 (2010).
[18] P.G. Sharov, I.A. Egorova, L.V. Grigorenko, *Phys. Rev. C* **90**, 024610 (2014).
[19] M.S. Golovkov *et al.*, *Phys. Lett. B* **672**, 22 (2009).
[20] S.I. Sidorchuk *et al.*, *Phys. Rev. Lett.* **108**, 202502 (2012).
[21] M.S. Golovkov *et al.*, *Phys. Rev. C* **76**, 021605(R) (2007).
[22] P.G. Sharov *et al.*, *Phys. Rev. C* **96**, 025807 (2017).
[23] Ł. Janiak *et al.*, *Phys. Rev. C* **95**, 034315 (2017).